

**CHARACTERIZING THE ROLE OF CLAUDIN-5 IN**  
**SKELETAL MUSCLE FIBROSIS AND**  
**CARDIOMYOPATHY**

**Undergraduate Honors Thesis**

**Jennifer Marie DeSalvo**

April 17, 2015

School of Health and Rehabilitation Sciences  
Biomedical Science Major

Dr. Jill A. Rafael-Fortney, Advisor  
Rafael-Fortney Laboratory  
Department of Molecular and Cellular Biochemistry  
The Ohio State University College of Medicine

**Contents**

<b>I. Acknowledgements.....</b>	<b>3</b>
<b>II. Vita.....</b>	<b>4</b>
<b>III. Abstract.....</b>	<b>5</b>
<b>IV. List of Tables and Figures.....</b>	<b>7</b>
<b>V. Introduction.....</b>	<b>8</b>
<b>VI. Methods.....</b>	<b>12</b>
<b>VII. Results.....</b>	<b>24</b>
<b>VIII. Discussion.....</b>	<b>43</b>
<b>IX. Conclusion.....</b>	<b>48</b>
<b>X. References.....</b>	<b>49</b>

## **I. Acknowledgements**

I would like to acknowledge multiple people for their assistance, support, and mentorship throughout my undergraduate career. First, I want to thank Dr. Jill Rafael-Fortney, for her constant guidance and encouragement in which I have learned the importance of perseverance, creativity, and resiliency. Her dedication to helping improve my skills as a researcher has reaffirmed my desire to become a physician-scientist passionate about combining medicine and research to improve patient care. I want to thank Dr. Paul Janssen and his laboratory, particularly Dr. Mohammad Elnakish, for their expertise and collaboration on this project. I would also like to thank other members of the Rafael-Fortney laboratory for their assistance and support, including Dr. Dawn Delfin, Sarah Swager, Jori Chambers, Neha Rastoogi, Jeovanna Lowe, Lauren Chen, Jenny Lee, Eric Schultz, Kevin Schill, Jessica Chadwick, and Spencer Hauck. Additionally, I want to thank the Biomedical Science undergraduate program, namely, Dr. John Gunn, Lori Martensen, and Steven Mousetes for providing me with this opportunity and privilege.

I would also like to thank my parents, Michael and Wendy, and my siblings, Michael, Katharine, and David, for their continual love and faith in me. They have inspired my passion for science and calling to serve others through my pursuit of medicine and research, which has forever changed my life.

Finally, I want to thank my friends, who have served as my mentors, motivators, and supporters. They have provided with me the resources and drive necessary to assist me in striving to achieve my goals and dreams. I am eternally grateful for everyone who has helped me on this journey.

**II. Vita**

June 2011.....Magnificat High School

August 2012-present.....Undergraduate Research Assistant  
Rafael-Fortney Laboratory, Molecular and Cellular Biochemistry,  
The Ohio State University College of Medicine

May 2013-July 2013.....American Heart Association Research Fellow

May 2014-July 2014.....Honors and Scholars Undergraduate Research Office Fellow,  
The Ohio State University and Internal Medicine 'Grever' Undergraduate Intern

May 2015..... B.S. Biomedical Science, The Ohio State University

### **III. Abstract**

Our laboratory has identified reductions in the claudin-5 protein in investigations of both a dystrophic cardiomyopathic mouse model and human cardiomyopathy.

Therefore, it is crucial to study the effects of isolated claudin-5 reductions in a claudin-5 knockdown (CKD) mouse model to determine whether loss of claudin-5 is sufficient to cause cardiomyopathy. Tamoxifen chow administration proved an effective method to knockdown claudin-5 expression in the myocardium while avoiding toxicity issues apparent with tamoxifen injections. Subsequent serial echocardiograms revealed that the experimental CKD mice exhibited initial physiological signs of a cardiomyopathic phenotype at 29 weeks of age. Immunofluorescence staining of these experimental mice also indicated a slight reduction and irregular staining patterns in the levels of claudin-5 and other cardiomyocyte membrane-extracellular matrix proteins. However, hematoxylin and eosin staining showed no signs of dilation or damage to the myocardium, indicating the lack of a cardiomyopathic phenotype at this timepoint. Furthermore, a dobutamine stress test did not induce a cardiomyopathic phenotype in experimental mice. This indicated the need to perform longitudinal echocardiograms with and without stress in future experiments to determine if these experimental mice develop cardiomyopathy as a result of claudin-5 reductions.

Our laboratory also seeks to determine if claudin-5 ectopic expression is capable of maintaining the structural integrity of skeletal muscles in a dystrophin-deficient mouse model. Immunofluorescence staining of claudin-5 confirmed that dystrophin-deficient skeletal muscle inoculated with a rAAV6-claudin-5 vector containing  $5 \times 10^{11}$  viral genomes exhibited over 70% claudin-5-expressing fibers, and that only 22% of claudin-

5 expressing skeletal muscle fibers contained central nuclei, an indicator of damage, compared to 48% in untreated dystrophic control muscles. Because there is ongoing damage in the dystrophin-deficient mouse model, the muscle fibers observed with cumulative degeneration and regeneration cycles may have been damaged prior to claudin-5 ectopic expression. Though this experiment is most clinically relevant to DMD patients that have ongoing damage to their striated muscles, further studies will be able to delineate the timing of a claudin-5-based therapeutic treatment in order to prevent damage prior to onset, rather than halting damage after onset. This data and its future implications may identify claudin-5 as a potential novel therapeutic target for treating DMD.

#### **IV. List of Tables and Figures**

<b>Figure 1.</b> Schematic representation of claudin-5 floxed construct in CKD mouse genome.....	13
<b>Table 1.</b> CKD mice groups and treatments.....	17
<b>Table 2.</b> List of immunofluorescent antibodies.....	19
<b>Table 3.</b> <i>Mdx</i> mice groups and treatments.....	22
<b>Figure 2.</b> PCR analysis of claudin-5 excision comparing tamoxifen chow and tamoxifen injection administration in CKD mice.....	25
<b>Figure 3.</b> Immunohistochemical staining of CKD mice myocardia at 14 weeks of age..	27
<b>Figure 4.</b> Ejection fractions of CKD mice at 20, 25, and 29 weeks of age.....	29
<b>Figure 5.</b> Immunofluorescence staining of CKD mice myocardia at 29 weeks of age...	31
<b>Figure 6.</b> Composites of hematoxylin and eosin-stained CKD mice hearts at 29 weeks of age.....	32
<b>Figure 7.</b> Immunofluorescence staining of dobutamine-stressed CKD mice myocardia.....	34
<b>Figure 8.</b> Composites of immunohistochemically-stained dobutamine-stressed CKD mice hearts.....	35
<b>Figure 9.</b> Immunohistochemical staining of vector-treated and control <i>mdx</i> mice TA muscles.....	37
<b>Figure 10.</b> Composites of claudin-5 immunofluorescently-stained vector-treated <i>mdx</i> mice TA muscles at varying concentrations.....	39
<b>Figure 11.</b> Composites of immunofluorescently-stained vector-treated and control <i>mdx</i> mice TA muscles.....	41

## **V. Introduction**

### **Muscular Dystrophy**

Duchenne muscular dystrophy (DMD) is a neuromuscular disorder characterized by progressive degeneration of striated muscles. This disease is a X-linked recessive form of muscular dystrophy, affecting approximately 1 in 5,000 males and resulting in premature death around 25 years of age.<sup>8</sup> DMD is caused by a mutation in the gene coding for the protein dystrophin,<sup>7</sup> a cytosolic protein that links actin filaments to the extracellular matrix in striated muscle.<sup>2,7,10</sup> In the absence of this protein, DMD patients experience decreased structural integrity of muscle tissue and impaired contractile function.<sup>6,12</sup> Eventually, the muscle tissue begins to deteriorate and is replaced by adipose and connective tissue as a result of fibrosis.<sup>13</sup> This process leads to a weakening of the skeletal muscles, causing immobility and respiratory diseases because of the rapid degeneration of the limb muscles and diaphragm, respectively.<sup>2,3</sup> More importantly, 95% of DMD patients develop dilated cardiomyopathy, and heart failure is the cause of death in at least 25% of patients.<sup>3</sup> Though there is currently no cure for DMD, treatment is generally aimed at controlling the onset of symptoms to maximize the quality of life, which includes glucocorticoids, mineralocorticoid receptor antagonists, and ACE inhibitors, in addition to other therapies in clinical trials involving exon skipping and gene therapy.

### **Dilated Cardiomyopathy**

Dilated cardiomyopathy (DCM) is a common cause of heart failure in both DMD patients and the general population.<sup>3</sup> DCM is a cardiac disease that is primarily characterized by force reductions in the left ventricle. The reductions in force cause the cardiomyocytes of the left ventricle to stretch and become thinner, resulting in dilation of the myocardium. Dilation causes the myocardium to weaken and eventually remodel, which manifests as cardiac chamber wall thinning and changes in chamber geometry to a more spherical, less elongated shape. The remodeling process causes a continuous decline in ejection fraction, the blood volume pumped out of the left ventricle with each heartbeat, and this prevents the heart from adequately



supplying the body's tissues and organs with enough blood. Over time, this condition can cause heart failure. Whereas the effects of DCM have been identified, the mechanism of DCM remains unknown.

### Claudin-5

Our laboratory has recently identified claudin-5 as a protein that becomes reduced early in the progression of DCM.<sup>3</sup> Claudin-5 is a transmembrane protein found as a component of tight junctions. In cardiac muscle, claudin-5 is localized at membrane-matrix junctions, linking the lateral cardiomyocyte membrane to the extracellular matrix. Loss of cardiac membrane-matrix interactions can contribute to the remodeling that manifests in DCM and heart failure.<sup>10</sup> Because claudin-5 is localized to the membrane-matrix junction, a decrease in claudin-5 could result in weak membrane-matrix binding, ultimately leading to the development of DCM.<sup>10</sup> Despite the reduction in claudin-5, the levels of other structural proteins remain unaltered,<sup>9</sup> suggesting that alterations in claudin-5 levels may represent a critical step in DCM progression.

### Role of Claudin-5 in Dilated Cardiomyopathy

Several studies performed in our laboratory have suggested that reductions in claudin-5 contribute to cardiac dysfunction during the early stages of the progression of DCM. Reduced claudin-5 levels were first correlated with DCM using a dystrophic cardiomyopathic mouse model. Compared to mice with a mild cardiomyopathy, reduced claudin-5 levels were observed in cardiac tissue from dystrophic cardiomyopathic mice via mRNA microarray analysis.<sup>11</sup> To further characterize the relationship between claudin-5 and DCM, my laboratory conducted a claudin-5 rescue experiment in this dystrophic cardiomyopathic mouse model. My laboratory showed that sustained claudin-5 levels in these mice prevented physiological and histological signs of cardiac dysfunction.<sup>3</sup> To investigate the relevance of reduced claudin-5 levels to human DCM, claudin-5 levels were compared in heart tissue from normal patients and patients with heart failure.<sup>9</sup> Claudin-5 levels were reduced in 60% of patients with heart failure, and this was independent of whether patients had muscular dystrophy-related DCM.<sup>7</sup> These studies suggest

that reduced claudin-5 levels may be involved in cardiomyopathy regardless of etiology.<sup>9</sup>

Though reduced claudin-5 levels have been correlated with DCM, these studies aim to identify a direct link between loss of claudin-5 and development of DCM.

### Significance

Heart disease is the leading cause of death in the United States. It often remains undiagnosed and end-stage heart disease is incurable. The study of DCM is significant because it is a common cause of heart failure that affects a large population, resulting in 50,000 hospitalizations a year and over 10,000 deaths in the United States alone.<sup>4,14</sup> Despite its prevalence, the mechanisms leading to DCM are unknown; therefore, it is crucial to discover novel pathways involved in the development of DCM. The proposed studies could identify loss of claudin-5 as a necessary step in DCM and determine how claudin-5 reductions are involved in the larger patient population. The information from these experiments could also be used to establish the potential therapeutic value of claudin-5. Restoring claudin-5 levels could be used to prevent further cardiomyocyte damage and potentially improve the condition of the heart in patients suffering from DCM.<sup>7</sup>

### Research Aims

The purpose of the first aim was to determine if a reduction in claudin-5 is sufficient to cause cardiac dysfunction characteristic of DCM. Claudin-5 reductions are present in cardiac tissue in investigations of both a dystrophic cardiomyopathic mouse model and human cardiomyopathy patients, suggesting that claudin-5 may be the cause of cardiac dysfunction during the development of DCM. This aim utilized claudin-5 knockdown (CKD) mice to determine whether a direct link exists between reduced cardiac claudin-5 levels and cardiac dysfunction associated with DCM. We hypothesized that reductions in claudin-5 in cardiomyocytes would compromise cardiac muscle function and morphology in the CKD mouse model. To address this aim, the effects of claudin-5 reductions in relation to cardiomyopathy in a

CKD mouse model were investigated in order to define the physiological, cellular, and molecular mechanisms of DCM resulting from loss of claudin-5.

The purpose of the second aim was to determine if upregulating claudin-5 levels is also capable of maintaining the structural integrity of skeletal muscle in a dystrophin-deficient mouse model. Our laboratory previously demonstrated that sustaining claudin-5 expression via delivery from a gene therapy vector prevented cardiac dysfunction and histopathology in utrophin-deficient dystrophic mice, supporting that claudin-5 may represent a therapy for patients suffering from DMD. We hypothesized that claudin-5 ectopic expression would help compensate for dystrophin-deficiency in skeletal muscle, by replacing missing muscle membrane-extracellular matrix linkages. To address this aim, claudin-5 was delivered to dystrophin-deficient skeletal muscle via rAAV6-claudin-5 vector to transduce a majority of muscle fibers in the tibialis anterior (TA) muscle located in the anterior compartment of the lower hind limb, which is in ideal position for needle injections.

## **VI. Methods**

### **Methods for Aim 1: To determine whether claudin-5 reduction in cardiomyocytes is sufficient to cause cardiomyopathy.**

#### **Animal Design**

##### **MerCreMer-Lox System**

My laboratory developed a claudin-5 knockdown (CKD) mouse model using the MerCreMer-Lox system to specifically and inducibly reduce claudin-5 in a cardiac tissue-specific knockdown. This mouse model was designed to excise the single claudin-5 exon from chromosome 16 in cardiomyocytes.<sup>12</sup> These mice contain two loxP sites that flank the single claudin-5 exon ("floxed"). This system utilizes a transgene that expresses a cre recombinase protein. This enzyme binds to the loxP sites and causes homologous recombination through inversion, deletion, or translocation to excise the claudin-5 exon. After the creation of the floxed construct, it was transfected into 129SV mouse embryonic stem cells. A neomycin antibiotic resistance cassette (Neo) was also contained in the floxed construct, and neomycin-resistant cells that contained the floxed construct were later implanted into the blastocytes of pregnant mice. The neomycin antibiotic resistance cassette was flanked by two frt sites to allow for removal of the neomycin cassette via the flp recombinase protein. Therefore, mice that contained the floxed claudin-5 construct with Neo flanked by frt sites were bred with mice expressing flp recombinase to remove the Neo cassette. To create the CKD experimental mice, mice that expressed the floxed construct without the Neo cassette and flp transgene were bred with mice that expressed cre recombinase. The cre recombinase was driven by the cardiomyocyte-specific promoter alpha myosin heavy chain 6 and was flanked by two mutated estrogen responsive elements (MerCreMer). These Mer elements were created to respond only to non-endogenous estrogen agonists, such as tamoxifen, and therefore, prevent cre recombinase from entering the nucleus of the cell in the presence of endogenous estrogen. When tamoxifen is present, cre recombinase enters the nuclei in cardiomyocytes and causes

recombination between the loxP sites in chromosome 16, excising the claudin-5 exon and preventing subsequent protein expression in the myocardium only.<sup>10</sup> The mice that expressed cre recombinase and flp recombinase were purchased from The Jackson laboratory.

#### Targeted allele

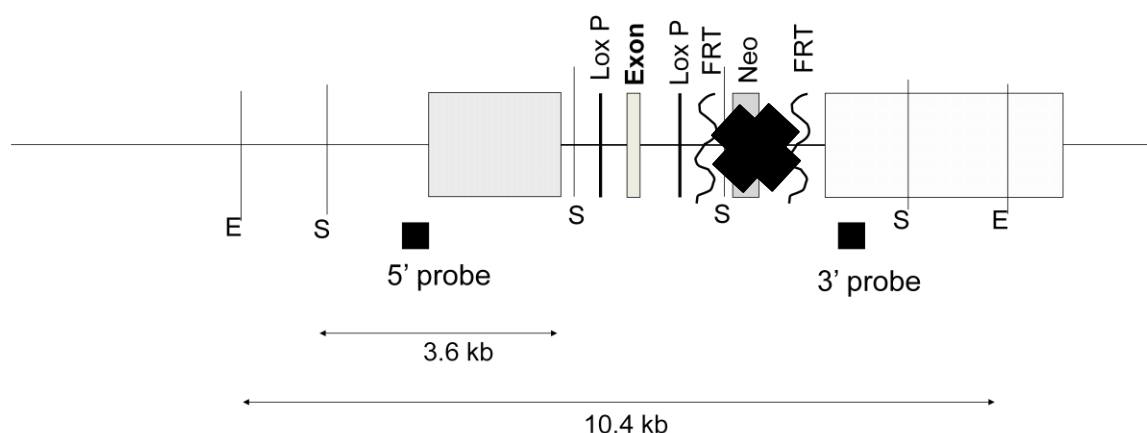


**Figure 1.** Schematic representation of the claudin-5 floxed allele that would be found in experimental mice after the homologous recombination event. The single claudin-5 exon is flanked by two loxP sites at the 5' and 3' ends. The neomycin antibiotic resistance cassette is flanked by two frt sites at the 5' and 3' ends. Mice possessing the floxed claudin-5 construct with Neo were bred with mice expressing flp recombinase to remove the Neo cassette, represented by the black "X." Mice without the Neo cassette and flp transgene were bred with that expressed cre recombinase. These experimental mice were then treated with tamoxifen to generate a cardiac-specific knockdown using the MerCreMer-Lox system.

The creation of a knockdown strain was necessary because a claudin-5 knockout in floxed/floxed mice without the neomycin cassette was found to be preneonatal lethal. The claudin-5 exon is 2.1 kilobases upstream from the first exon of CDC45, a gene required for postimplantation mouse development, and deletion of neomycin from the 3' intron could affect the CDC45 gene and result in neonatal death of floxed/floxed mice.

Experimental heterozygous claudin-5 flox+/- mice that contain cre (Cldn5 flox+/-; cre+/-, referred to as het cre+) often exhibited reduced claudin-5 levels in the myocardium at membrane-matrix junctions after tamoxifen administration compared to wild-type mice that do not contain cre (Cldn5 flox-/-; cre-/-, or wt cre-).<sup>7</sup> Similar reductions in claudin-5 are observed in

other animal models and human patients with cardiomyopathy, suggesting that the CKD mouse model may represent a clinically-relevant animal model of cardiomyopathy. Het cre- (heterozygous *Cldn5* flox+/-; cre-/-) and wt cre+ (*Cldn5* flox-/-; cre+/-) mice were also bred for use as experimental controls for the floxed claudin-5 allele and for the presence of cre.

### Breeding

All animals were mated and kept in accordance with a protocol approved by the Institutional Animal Care and Use Committee at The Ohio State University. Het cre+ mice were bred with wt cre- mice. This breeding scheme produced litters with half heterozygous mice and half wild-type mice. It also produced litters with half cre+ and half cre- mice. This provided a variety of controls for the experimental het cre+ mice.

### DNA Extraction

At three weeks of age, one centimeter of tail was snipped from the mice and suspended in 600  $\mu$ l of TNES buffer (0.5 M Tris-HCl pH 7.5, 5 M NaCl, 0.5 M EDTA, 10% sodium dodecyl sulfate) and 17.5  $\mu$ l of 20 mg/ml proteinase K to incubate at 55°C overnight. An additional 50  $\mu$ l of proteinase K was added to tails that had not fully digested in the overnight incubation. Upon complete digestion of the tail, 167  $\mu$ l of 5 M NaCl was added to each tube and the tubes were shaken for 15 seconds. The tubes were then centrifuged for 10 minutes at 4°C at 14,000 rpm. The supernatant was poured into a new tube and 800  $\mu$ l of 100% cold ethanol was added to each tube and mixed. The DNA was spooled onto the sealed end of a Pasteur pipette and rinsed in 70% ethanol. The DNA was then resuspended in 300  $\mu$ l 1X TE buffer (10 mM Tris-HCl pH 8.0, 1 mM EDTA) and incubated for 10 minutes at 65°C. The DNA was stored in this buffer at 4°C.

### Polymerase Chain Reaction

Polymerase chain reaction (PCR) was used to identify genotypes for appropriate breeding mice and experimental analysis. At three weeks of age, one centimeter of tail was

snipped from the mice and digested to extract DNA for genotyping according to the standard salt-out extraction protocol as previously described. PCR reactions were conducted using the CreER primers (Forward: CCGGTCGATGCAACGAGTGAT, Reverse: ACCAGAGTCATCCTTAGCGCC, 59°C annealing temperature), 5'LoxP primers (Forward: ACCAGAGTCATCCTTAGCGCC, Reverse: CGAAGTTATTAGGTCCCTCGACC, 62°C annealing temperature), and wildtype primers (Forward: GGAGAAGAACCTACTGAACCAAAGG, Reverse: TCACCCAAGTTGCCATTCCC, 59°C annealing temperature). These primers were designed to detect the presence of the cre transgene, the floxed construct, and the wildtype product, respectively. The PCR reaction contained 7.5 µl 2X Syzygy Taq master mix, 0.3 µl forward primer, 0.3 µl reverse primer, 5.9 µl distilled water, and 1 µl of DNA. ΦX HaeIII was used as the molecular weight marker. PCR products were separated by gel electrophoresis on 2% agarose gels and visualized via ultraviolet light. The presence of a PCR product at 798 base pairs (bp) using the CreER primers indicated the presence of the cre recombinase gene. The presence of the 5'loxP product was determined by the presence of a ~600 bp product when the reaction was run with 5'loxP primers. This product indicated that at least one allele contained the 5'loxP construct. A wildtype primer reaction was used to determine the presence of the wildtype allele, with the wildtype product present at ~550 bp. Heterozygous mice show two products, one for the wildtype product and a longer one for the 5'loxP product.

PCR was also utilized to determine if tamoxifen chow-treated mice excised the claudin-5 exon. Hearts were dissected from experimental het cre+ mice and a small portion of the heart was digested to isolate DNA for PCR analysis. The standard salt-out extraction protocol outlined above was followed with primers designed to detect the presence of the floxed construct. PCR products that appeared at 2027 bp denoted the presence of the large floxed construct in the myocardium of the tamoxifen-treated mice, indicating incomplete excision of the claudin-5 exon.

PCR products that appeared at 564 bp revealed deletion of the floxed construct in the myocardium of the tamoxifen-treated mice, indicating complete excision of the claudin-5 exon.

#### *Tamoxifen Injection*

At 4 weeks of age, het cre+ male and female mice and all genotypes of controls (wt cre+, wt cre-, het cre-) (Group A, n=75) were injected with tamoxifen (Sigma) dissolved in corn oil at 20 mg/ml. The mice were administered 200 mg/kg per day of tamoxifen per body weight. Tamoxifen was administered via intraperitoneal injection for 5 consecutive days.

#### *Tamoxifen Chow*

Due to toxicity issues, tamoxifen administration switched from injections to chow. Tamoxifen chow contained 400 mg/g of tamoxifen citrate/kg Teklad Global 16% Protein Rodent Diet at an estimated dose of approximately 40 mg/kg per day for two consecutive weeks, which was administered beginning at four weeks of age to het cre+ male and female mice and all genotypes of controls (wt cre+, wt cre-, het cre-) (Group B-E, n=93).

#### *Experimental Design*

To induce excision of the claudin-5 exon via the most efficient administration of tamoxifen, Group B was treated with tamoxifen chow for 2 weeks starting at 4 weeks of age and compared to the Group A mice that were treated with tamoxifen injections for 5 consecutive days beginning at 4 weeks of age. This experimental design was intended to demonstrate whether tamoxifen chow excised the claudin-5 exon and eliminated toxicity issues apparent with tamoxifen injections in the CKD mouse model.

After confirming successful excision of the claudin-5 exon via tamoxifen chow treatment, all male and female mice from Groups C-E were treated with tamoxifen chow for 2 weeks starting at 4 weeks of age to induce deletion of the claudin-5 exon. Primary comparisons were



performed in het cre<sup>+</sup> and wt cre<sup>-</sup> mice. However, tamoxifen-treated het cre<sup>-</sup> and wt cre<sup>+</sup> were also included to control for the floxed claudin-5 allele and for the presence of cre.

**Table 1.** CKD mice groups and treatments.

<b>Group</b>	<b>Mice used</b>	<b>Treatment</b>	<b>Purpose</b>	<b>Age at death (weeks)</b>
A (n=75)	Experimental: het cre <sup>+</sup> Control: wt cre <sup>-</sup> , wt cre <sup>+</sup> , het cre <sup>-</sup>	Tamoxifen injections	To identify cardiomyopathic phenotype	14
B (n=10)	Experimental: het cre <sup>+</sup> Control: wt cre <sup>-</sup> , wt cre <sup>+</sup> , het cre <sup>-</sup>	Tamoxifen chow	To compare the efficiency of claudin-5 excision to tamoxifen injections	8
C (n=37)	Experimental: het cre <sup>+</sup> Control: wt cre <sup>-</sup> , wt cre <sup>+</sup> , het cre <sup>-</sup>	Tamoxifen chow	To identify cardiomyopathic phenotype	14
D (n=26)	Experimental: het cre <sup>+</sup> Control: wt cre <sup>-</sup> , wt cre <sup>+</sup> , het cre <sup>-</sup>	Tamoxifen chow	To conduct serial echocardiograms to identify cardiomyopathic phenotype	29
E (n=15)	Experimental: het cre <sup>+</sup> Control: wt cre <sup>-</sup> , wt cre <sup>+</sup> , het cre <sup>-</sup>	Tamoxifen chow	To conduct dobutamine stress test to identify cardiomyopathic phenotype	25

## **Assays**

### **Echocardiograms**

Dr. Mohammad Elnakish from Dr. Paul Janssen's laboratory performed serial echocardiograms on Group C at 14 weeks of age, Group D at 20, 25, and 29 weeks of age, and Group E at 25 weeks of age to determine ejection fractions and calculate left ventricle mass/body weight ratios.

### **Dobutamine**

Jori Chambers, Lauren Chen, and Jenny Lee from the Rafael-Fortney Laboratory at The Ohio State University College of Medicine conducted a dobutamine stress test on Group E mice at 20 weeks of age to investigate the effects of reduced claudin-5 on whole heart function following  $\beta$ -adrenergic stimulation. Each mouse was intraperitoneally injected with dobutamine ( $20 \mu\text{m/g}_{\text{body weight}}$ ) diluted in 0.9% saline twice daily for seven days. On the seventh day, cardiac function was assessed via echocardiography. Mice were then monitored continuously for the first hour and at twenty-minute intervals for nine hours. No acute cardiac death was observed in all genotypes of mice after 48 hours following the seventh dobutamine injection. Mice were dissected and cardiac tissue was harvested as detailed below. Damage to the myocardium was visualized by immunohistochemical staining under brightfield and fluorescent microscopy.

### Dissections

Group C mice were dissected at 14 weeks of age and Group D mice were dissected at 29 weeks of age to assess the severity of cardiac damage due to loss of claudin-5. A blood sample was obtained and centrifuged to collect serum. The heart was removed and cut transversely into two sections. The inferior half was embedded in optimal cutting temperature (OCT) medium and frozen on liquid nitrogen-cooled isopentane for histological sectioning while the superior half was frozen in liquid nitrogen for subsequent protein and DNA isolation. The quadriceps muscle was removed and cut transversely, and one section was frozen in liquid nitrogen and the other was frozen in OCT for sectioning. The lungs, liver, and kidney were removed and frozen in liquid nitrogen. Tissue samples embedded in OCT were cut into  $8 \mu\text{m}$  sections using a cryostat, mounted on slides, and stored at  $-80^\circ\text{C}$ .

### Tissue Analysis

#### *Immunofluorescence*

Heart sample slides were warmed to room temperature and the sections were encircled with a hydrophobic pen. The slides were equilibrated in a potassium phosphate buffered solution (KPBS:  $\text{K}_2\text{HPO}_4$ ,  $\text{KH}_2\text{PO}_4$ ,  $\text{NaCl}$ ) for five minutes. They were blocked with KPBS +1% gelatin for

fifteen minutes and rinsed with KPBS for five minutes. The slides were incubated in 100  $\mu$ L of a primary antibody (see Table 2) for two hours at room temperature in a humid chamber. The antibody was diluted to its optimal dilution with KPBSG (KPBS + 0.2% gelatin) and 1% normal goat serum (NGS). The slides were rinsed for five minutes three separate times in KPBSG. The slides were then incubated in 100  $\mu$ L of a secondary antibody for one hour at room temperature in a wet chamber in the absence of light. The secondary antibody was diluted to its optimal dilution with KPBSG and NGS. The slides were washed with KPBSG for five minutes three separate times. Each slide was mounted with 35  $\mu$ L of a solution of vectashield and DAPI, which stains nuclei, (at 2  $\mu$ L/ml) and coverslipped. The slides were stored in a -20°C frost-free freezer. These sections were visualized and photographed at fixed exposure times on a Nikon Eclipse 800 Microscope with an epifluorescent mercury lamp using a SPOT camera and software. Images of each antibody stain were taken at the same exposure for each experiment to ensure consistency between samples.

**Table 2.** Primary\* and secondary\*\* antibodies used for immunofluorescent staining.

<b>Antibody (Species)</b>	<b>Company</b>	<b>Dilution</b>	<b>Other Specifications</b>
Claudin-5* (Rabbit)	Acris	1:750	None
Ephrin B1* (Goat)	R&D Systems	1:25	Fetal Bovine serum used instead of NGS
Collagen* (Rabbit)	Abcam	1:100	None
Fibronectin* (Rabbit)	Abcam	1:40	None
Immunoglobulin G** (Mouse)	Invitrogen	1:100	None

### *Hematoxylin and Eosin Staining*

Heart tissue samples were also stained with hematoxylin, which stains nuclei, and eosin, which stains cytosol and extracellular material, to visualize the overall morphology of the myocardium. The slides were stained using a standard protocol with appropriate ethanol dehydration steps. The slides were fixed with 100% ethanol for 30 seconds at room temperature

and subsequently washed in tap water. The slides were then stained with hematoxylin for 30 seconds and washed in tap water. The slides were stained with eosin for 20 seconds and washed in tap water. They were then dehydrated in 100% ethanol, 90% ethanol, and 70% ethanol and washed with histochoice clearing agent. The slides were mounted with cyto seal and coverslipped. The slides were then visualized on a light microscope and images were taken using Advanced Spotware technology. Individual pictures taken at 4X magnification were composited using Adobe PhotoShop.

**Methods for Aim 2: To determine whether claudin-5 expression helps protect skeletal muscle from the degenerative effects of dystrophin-deficiency.**

**Animal Design**

The *mdx* (*Dmd*<sup>*mdx*</sup>; *utrn*<sup>+/+</sup>) model is a murine model of DMD, which arises from a spontaneous mutation in the dystrophin gene. *Mdx* mice, like DMD patients, lack dystrophin and have previously been identified to exhibit mild skeletal muscle fibrosis and mild cardiomyopathy. Therefore, this mouse model is appropriate for testing therapeutic intervention at the early stages of disease.

*rAAV-claudin-5 vector*

A recombinant AAV6-claudin-5 vector carrying a mouse claudin-5 cDNA expressed from a minimal cytomegalovirus promoter (rAAV6-claudin-5; 1 x 10<sup>11</sup> viral genomes) was designed to deliver claudin-5 to skeletal muscles. This rAAV6 vector has previously been shown to confer sustained expression of the delivered gene product within 2 weeks of a single intravenous injection.<sup>2</sup>

*Intramuscular injection*

Prior to the muscle injection, each mouse was anesthetized via the nose cone method. During the initial induction stage, oxygen flow was 2 liters/minute with 5% isoflurane. Once reflexes became absent and mouse respirations became slow, shallow breaths, oxygen flow was reduced to 0.8 liters/minute with 2% isoflurane to maintain loss of consciousness. One drop of Nair was applied to the right leg and removed with a non-woven sponge. It was washed with PBS and 100% ethanol to prevent skin irritation. A syringe (3/10 cc U-100 Insulin syringe) was loaded with 30 µl of sterile PBS and the needle (30G x 3/8 inch needle) was bent to 90° angle. The needle was then injected into the TA muscle belly near the junction of TA and extensor digitorum longus (EDL) muscles. These steps were repeated with injection of the virus into the left leg. The isoflourane and oxygen were removed following injections, and the mouse was monitored for movement and normal, rapid breaths.

### **Experimental Design**

Four-week-old weaned male and female *mdx* mice (Group 1; n=5), which exhibit histological and physiological signs of skeletal muscle pathology, were injected with a rAAV6-claudin-5 vector at  $1 \times 10^{11}$  viral genomes (vg) in phosphate-buffered saline (PBS) via intramuscular injection into the TA muscle. To control for the mechanics of injecting the mice and to compare the normal protein levels of claudin-5 for experiments, the contralateral TA muscle was injected with an equivalent volume (30  $\mu$ l) of PBS.

Titration experiments were performed with the goal of achieving complete transduction of claudin-5 in skeletal muscle fibers. rAAV6-claudin-5 was tested at  $5 \times 10^{11}$  and  $1 \times 10^{12}$  vg in *mdx* mice (Group 2; n=2).

Upon confirmation that rAAV6-claudin-5 transduced more than 50% of skeletal muscle fibers, the vector was administered at  $5 \times 10^{11}$  vg to additional *mdx* mice (Group 3; n=5).

**Table 3.** *Mdx* mice groups and treatments.

<b>Group</b>	<b>Mice used</b>	<b>Treatment (via TA muscle injections)</b>	<b>Purpose</b>	<b>Age at death (weeks)</b>
1	5	rAAV6-claudin-5 vector at $1 \times 10^{11}$ vg and PBS	To determine if claudin-5 ectopic expression helps compensate for dystrophin- deficiency in skeletal muscle	8
2	2	rAAV6-claudin-5 vector at $5 \times 10^{11}$ vg and $1 \times 10^{12}$ vg	To achieve complete transduction of claudin-5 in skeletal muscle	8
3	5	rAAV6-claudin-5 vector at $5 \times 10^{11}$ vg and PBS	To achieve the purposes of Groups 1 and 2	8

## **Assays**

### *Dissections*

*Mdx* mice in Groups 1, 2, and 3 were dissected at 8 weeks of age to assess if claudin-5 ectopic expression helped compensate for dystrophin-deficiency in skeletal muscle. The TA, EDL, and quadriceps muscles were removed and cut transversely into two sections. The superior half was embedded in OCT and frozen on liquid nitrogen-cooled isopentane for histological sectioning while the inferior half was frozen in liquid nitrogen for protein isolation. Tissue samples embedded in OCT were cut into 8  $\mu$ m sections using a cryostat, mounted on slides, and stored at -80°C.

### *Immunofluorescence*

As described for Aim 1.

### *Hematoxylin and Eosin Staining*

As described for Aim 1.

### *Central Nuclei Quantification*

*Mdx* mice TA muscles treated with rAAV6-claudin-5 in Groups 1, 2, and 3 were immunofluorescently stained with a polyclonal claudin-5 antibody and pictures of merged claudin-5 and DAPI stains were taken at the same exposure time and magnification. Because central nuclei in skeletal muscle fibers are an indicator of previous damage and subsequent regeneration of the muscle fiber, the number of central nucleated claudin-5-expressing muscle fibers were calculated and analyzed as a percent of the total number of claudin-5 expressing fibers.

## **VII. Results**

### **Results for Aim 1: To determine whether claudin-5 reduction in cardiomyocytes is sufficient to cause cardiomyopathy.**

#### **A. Tamoxifen chow treatment was an effective method to excise the construct containing the single claudin-5 exon.**

Previous results showed that tamoxifen administration via injections to excise the construct containing the single claudin-5 exon in the CKD mouse model exhibited cre-dependent toxicity, which resulted in accelerated reduction of whole heart function in het cre<sup>+</sup> and wt cre<sup>+</sup> mice. As a result, tamoxifen was alternatively administered in a mouse chow at a lower dose and longer period of administration to alleviate the high toxic dose and invasiveness of tamoxifen injections. DNA from hearts of tamoxifen-injected (Group A) and tamoxifen chow-treated (Group B) mice at 14 weeks of age was isolated and amplified in PCR experiments to compare if the construct had been excised (Figure 2). The presence of the upper band at 2027 base pairs (bp), produced from a PCR reaction using primers surrounding the claudin-5 exon and loxP sites, indicated incomplete excision of the exon, whereas the presence of the lower band at 564 bp implied complete excision of the construct in het cre<sup>+</sup> mice. Analysis of this data showed successful excision of the construct in both tamoxifen-injected and tamoxifen chow-treated het cre<sup>+</sup> mice, indicating that tamoxifen chow treatment was as efficient as tamoxifen injections in excising the construct.



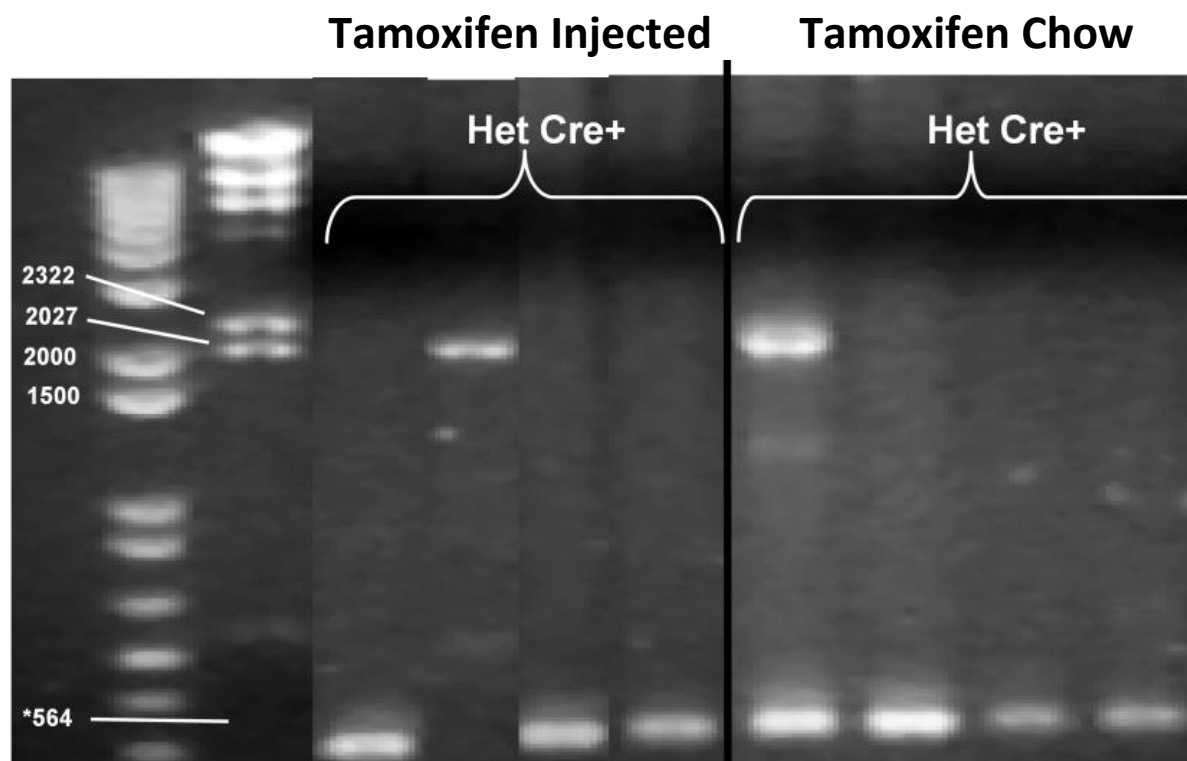


**Figure 2.** Example of PCR DNA product bands from genotyping experiments. \*Bands present at 564 bp indicated complete excision of the construct containing the claudin-5 exon, while bands present at 2027 bp indicated incomplete excision of the construct. PCR analysis indicated that mice treated with tamoxifen chow (two-week treatment at ~40 mg/kg per day) excised the construct, with similar success compared to mice injected with tamoxifen (five day treatment at 200 mg/kg per day).

**B. Experimental het cre+ mice exhibited no observable cardiomyopathic phenotype at 14 weeks of age.**

Because tamoxifen chow treatment successfully excised the construct containing the claudin-5 exon, mice of all four genotypes of the CKD model were treated with tamoxifen chow to knockdown the claudin-5 gene expression and determine the timepoint at which mice may develop DCM due to loss of claudin-5. Previous data showed that at 14 weeks of age, het cre+ mice did not exhibit an average ejection fraction within the range indicative of a cardiomyopathic phenotype (unpublished). These mice were dissected at 14 weeks of age, and their myocardium was harvested and studied using immunohistochemical stains. Immunofluorescence staining analysis (Figure 3) showed no significant changes in the levels of claudin-5 or ephrin B1, a membrane-matrix protein that interacts with claudin-5 in the myocardium. No significant

changes in the levels of collagen, an extracellular matrix protein, indicated the absence of collagen scarring, or gross increases in the amount of interstitial collagen, therefore demonstrating the presence of maintained structure and integrity of the myocardium.

Hematoxylin and eosin staining showed no major dilation of the left ventricle, necrosis of myocytes, or increased fibrosis that might indicate a cardiomyopathic phenotype. Thus, at 14 weeks of age, het cre + mice treated with tamoxifen chow showed no major reduction of claudin-5 levels or changes in cell pathology indicative of a cardiomyopathic phenotype.

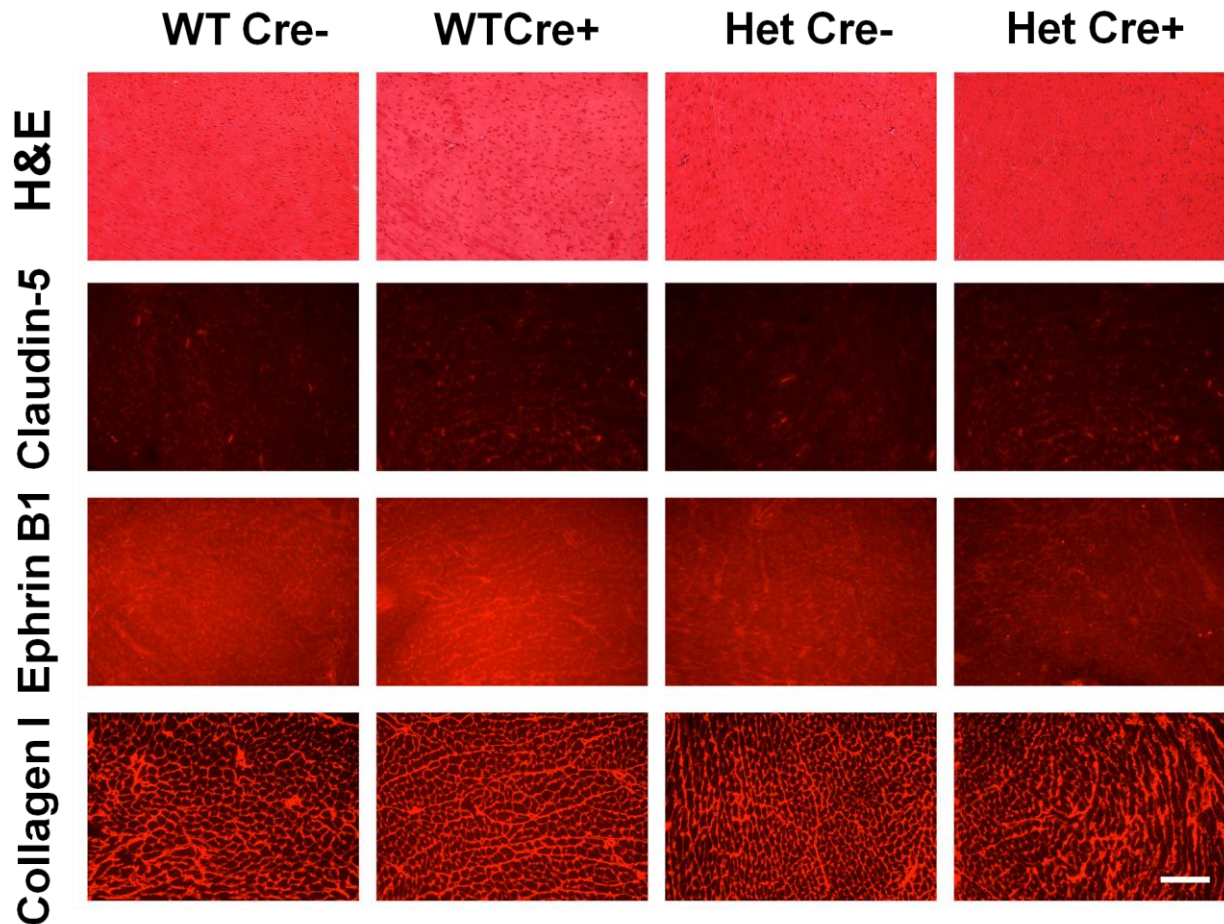


**Figure 3.** Immunohistochemical staining of heart sections of experimental mice and controls at 14 weeks of age. Immunohistochemical staining of het cre<sup>+</sup> mice at 14 weeks of age for these four markers (left axis) showed no major reduction of claudin-5 levels or changes in cell pathology in the myocardium in comparison of each genotype (top axis) to indicate the presence of a cardiomyopathic phenotype. Top row: Hematoxylin and eosin staining appeared consistent between the experimental het cre<sup>+</sup> mice (n=12) and control mice, wt cre<sup>-</sup> (n=7), wt cre<sup>+</sup> (n=13), and het cre<sup>-</sup> (n=10) and did not exhibit signs of dilation, necrosis of myocytes, or increased fibrosis indicative of a cardiomyopathic phenotype. Second row: Claudin-5 staining is not reduced when comparing immunostaining of het cre<sup>+</sup> experimental mice and control mice. Third row: Staining of experimental het cre<sup>+</sup> for ephrin B1, a membrane-matrix protein that interacts with claudin-5 in the myocardium, was not reduced compared to control mice. Bottom row: Collagen I staining showed no changes in the levels of collagen, an extracellular matrix protein, demonstrating the absence of collagen scarring and maintained cardiomyocyte membrane integrity. (Bar equals 100  $\mu$ m)

**C. Serial echocardiograms of het cre+ mice revealed initial physiological signs of a cardiomyopathic phenotype.**

Because no cardiomyopathic phenotype was observed at 14 weeks of age, another group of mice (Group D; n=26) was treated with tamoxifen chow and underwent serial echocardiograms at 20 weeks of age (Figure 4A), 25 weeks of age (Figure 4B), and 29 weeks of age (Figure 4C). At 20 weeks of age, het cre + mice had reduced ejection fractions of 57.3%, 56.4% at 25 weeks of age, and 54% at 29 weeks of age, which remained consistently slightly lower than the other genotypes (Figures 4A-C). Ejection fraction data was not significantly different based on treatment groups ( $P= 0.340$ ), length of time ( $P= 0.980$ ), or interactions between treatment groups and length of time ( $P= 0.504$ ) according to a 2-way ANOVA repeated measures. Because severe cardiac dysfunction has an average ejection fraction of 55% or lower, these het cre+ mice showed initial signs of a cardiomyopathic phenotype at 29 weeks of age.

Figure 4A. Group D Echoes at 20 weeks of age

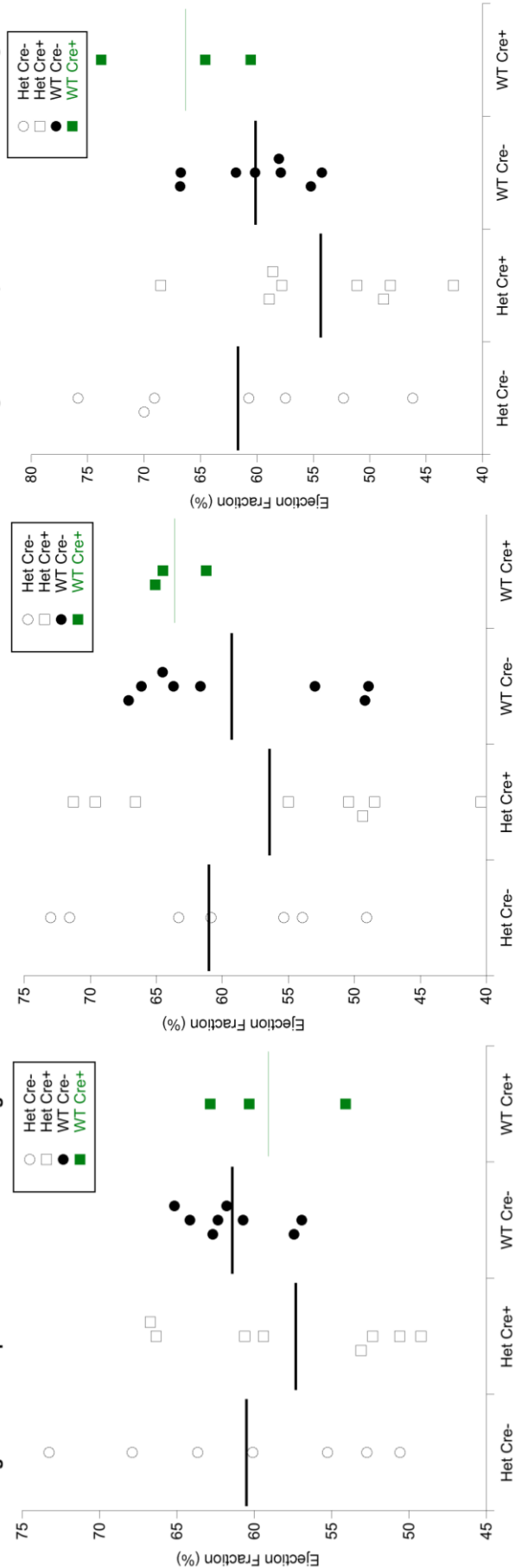


Figure 4B. Group D Echoes at 25 weeks of age

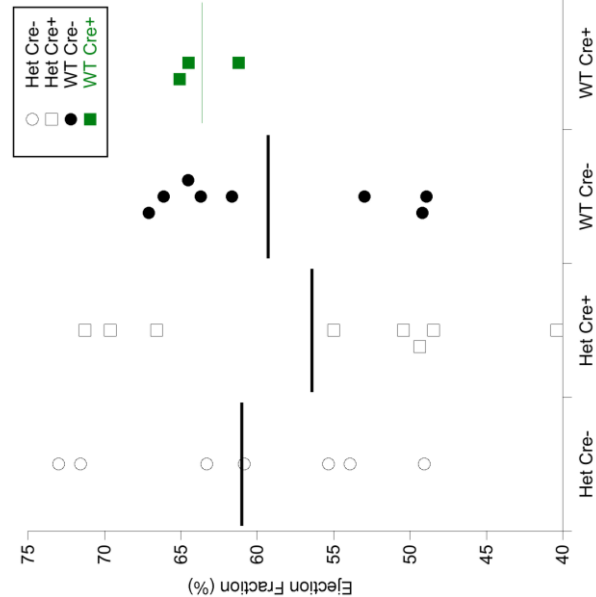
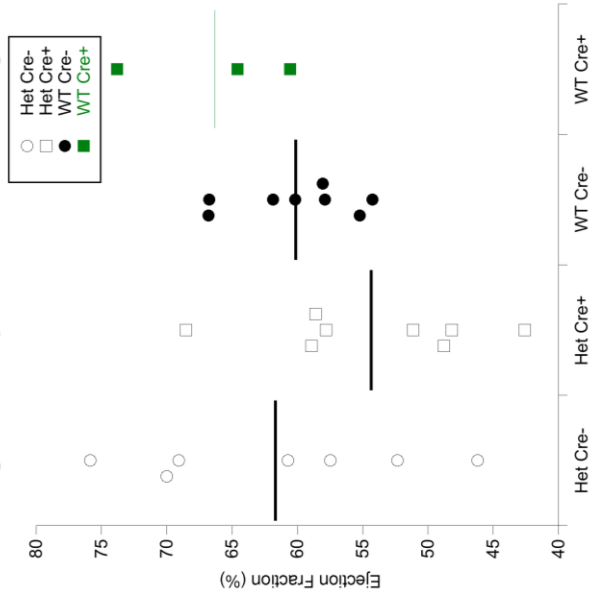
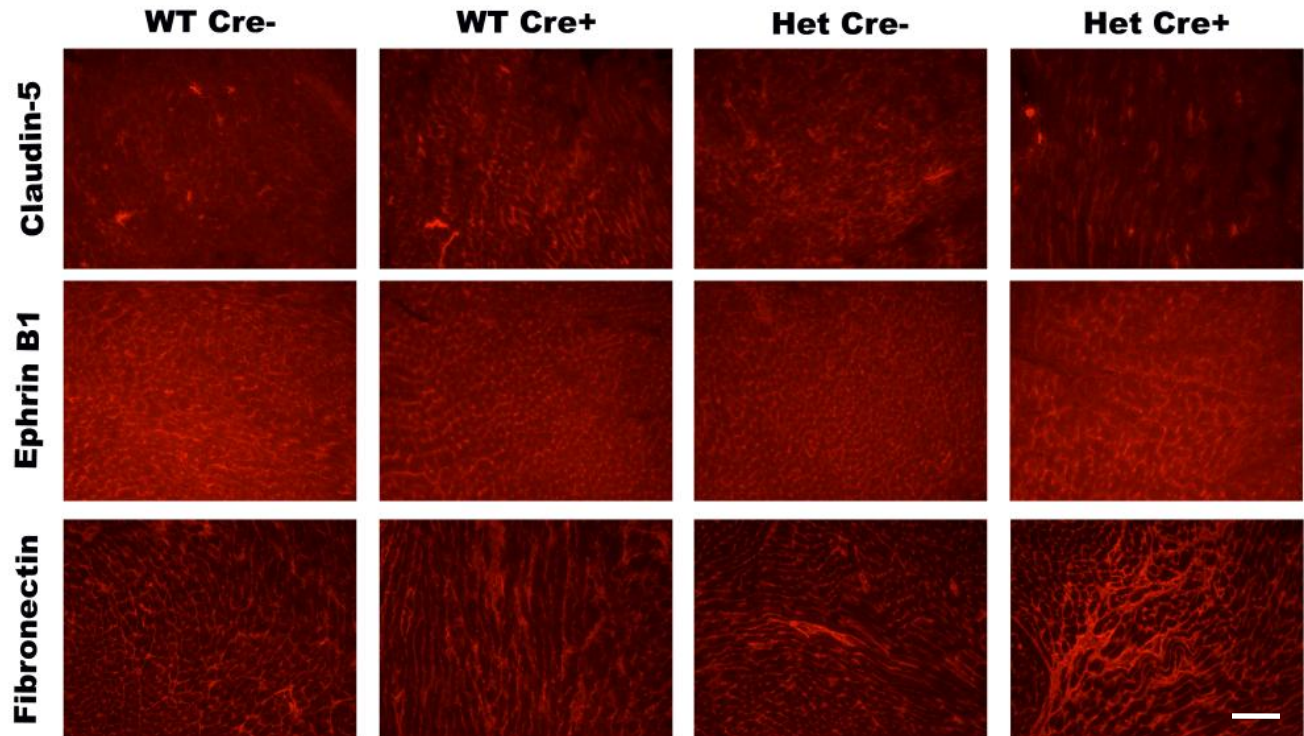


Figure 4C. Group D Echoes at 29 weeks of age



**Figures 4A-C.** Longitudinal echocardiogram average ejection fraction data. Experimental het cre+ mice (n=8) exhibit, on average (indicated by line), lower ejection fractions than each control group, wt cre- (n=8), wt cre+ (n=3), het cre- (n=7), at 20 weeks of age (4A), 25 weeks of age (4B), and 29 weeks of age (4C). Though a two-way ANOVA repeated measures test indicated that ejection fraction data was not significantly different based on treatment groups, length of time, or interactions between treatment groups and length of time, a trend of reduced ejection fractions over time in experimental het cre+ mice hearts was observed. Furthermore, experimental het cre+ mice at 29 weeks of age exhibited an average ejection fraction of 54%, which is in the clinical range of severe cardiac dysfunction, and indicated that these mice displayed initial signs of compromised cardiac function at this timepoint.

Group D mice were dissected at 29 weeks of age to determine if a reduction of claudin-5 was sufficient to cause histopathological signs of a cardiomyopathic phenotype that preceded physiological symptoms of DCM. Claudin-5 immunofluorescence staining of 29 week old CKD mouse hearts showed a slight reduction of claudin-5 in the cardiomyocyte membranes of het cre+ mice in a mosaic pattern (Figure 5), likely due to the stochastic nature of cre excision of the claudin-5 allele in the myocardium. Ephrin B1 immunofluorescence staining showed that ephrin B1 was similarly stained in a mosaic pattern in het cre+ mice, however, without a major observable loss of ephrin B1 expression. Fibronectin, an extracellular matrix protein similar to collagen I, revealed several irregular areas of increased fibronectin staining in het cre+. This indicated the presence of extracellular matrix proliferation and scarring in the myocardium, possibly resulting from claudin-5 reduction.



**Figure 5.** Immunofluorescence staining of heart sections of experimental mice and controls at 29 weeks of age. Top row: Claudin-5 staining is slightly reduced in the membranes of cardiomyocytes in a mosaic pattern in experimental het cre<sup>+</sup> mice (n=8) compared to wt cre<sup>-</sup> (n=8), wt cre<sup>+</sup> (n=3), and het cre<sup>-</sup> (n=7). Middle row: Ephrin B1 staining showed reduced ephrin B1 expression in experimental het cre<sup>+</sup> mice also in a mosaic pattern similar to claudin-5 staining (top row), compared to control mice. Bottom row: Fibronectin staining, an extracellular matrix protein, exhibited irregular patterns of staining in experimental het cre<sup>+</sup> mice, which indicated the presence of extracellular proliferation and scarring, possibly due to loss of claudin-5. (Bar equals 100µm)

Despite these changes in protein expression and reduction in ejection fractions in het cre<sup>+</sup> mice, hematoxylin and eosin staining of 29 week old CKD mouse hearts exhibited no signs of dilation or damage to the myocardium (Figure 6). This indicated a lack of a cardiomyopathic phenotype at this timepoint in het cre<sup>+</sup> mice. However, an additional group of mice are currently being studied to gather longitudinal echocardiogram data in order to determine the timepoint at which het cre<sup>+</sup> mice exhibit a significant reduction in ejection fraction as a result of loss of claudin-5.



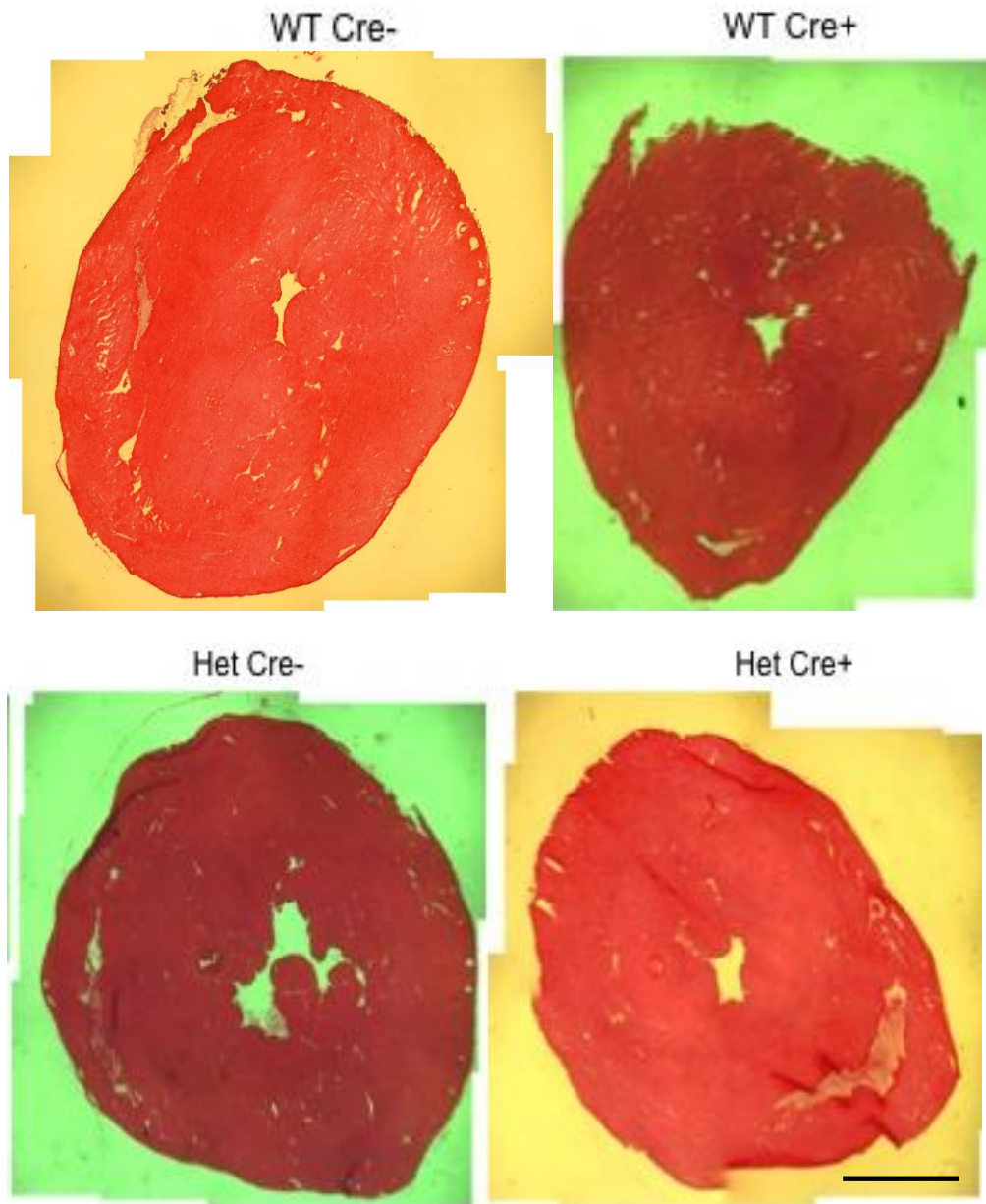


**Figure 6.** Histology of composited heart sections from experimental het cre+ mice and controls. Hematoxylin and eosin staining of transverse sections of left ventricles from experimental het cre+ mice hearts (n=8) at 29 weeks of age compared with control mice hearts, wt cre- (n=8), wt cre+ (n=3), and het cre- (n=7). Experimental het cre+ mice hearts showed no signs of dilation or damage to the myocardium characteristic of cardiomyopathy at 29 weeks of age. (Bar equals 1mm)



#### **D. Dobutamine stress test did not induce a cardiomyopathic phenotype in het cre+ mice.**

To test whether the CKD mice exhibit cardiomyopathy under stress, a group of CKD mice (Group E; n=15) were given serial injections of the  $\beta$ -adrenergic agonist dobutamine (20  $\mu\text{g/g}_{\text{body weight}}$  in 0.9% saline twice daily/1 week). Het cre+ mice at 25 weeks of age following dobutamine injections exhibited increased heart rates (462.06 beats/minute) compared to wt cre- mice (421.29 beats/minute; het cre-: 489.68 beats/minute; wt cre+: 423.83 beats/minute) and decreased ejection fractions (58.43%) compared to wt cre- mice (67.99%; wt cre+ 56.24%; het cre- 74.34%). These results also showed that 25 week old tamoxifen-treated het cre+ mice stressed with dobutamine (Group E) had slightly elevated ejection fractions compared to tamoxifen-treated 25 week old het cre+ mice (Group D), indicating that the dobutamine stress test did not induce a physiological cardiomyopathic phenotype in het cre+ mice.

These mice were dissected at 25 weeks of age to investigate the histopathological effect of claudin-5 reduction in the myocardium of dobutamine-stressed mice. Claudin-5 immunofluorescence staining showed a reduction of claudin-5 in the membranes of cardiomyocytes in a mosaic pattern compared to other genotypes (Figure 7). IgG immunofluorescence staining was used to detect serum IgG accumulation in the myocardium indicative of myocytes with membrane damage or regions of fibrosis. This showed several fibrotic regions (indicated by bright green) primarily in whole heart composites of het cre+ mice, indicating that loss of claudin-5 in dobutamine-stressed CKD mice may have resulted in damage to the myocardium (Figure 8, top row). Hematoxylin and eosin staining of het cre+ mice did not reveal any signs of dilation or damage to the myocardium (Figure 8, bottom row), indicating the lack of a histopathological cardiomyopathic phenotype.

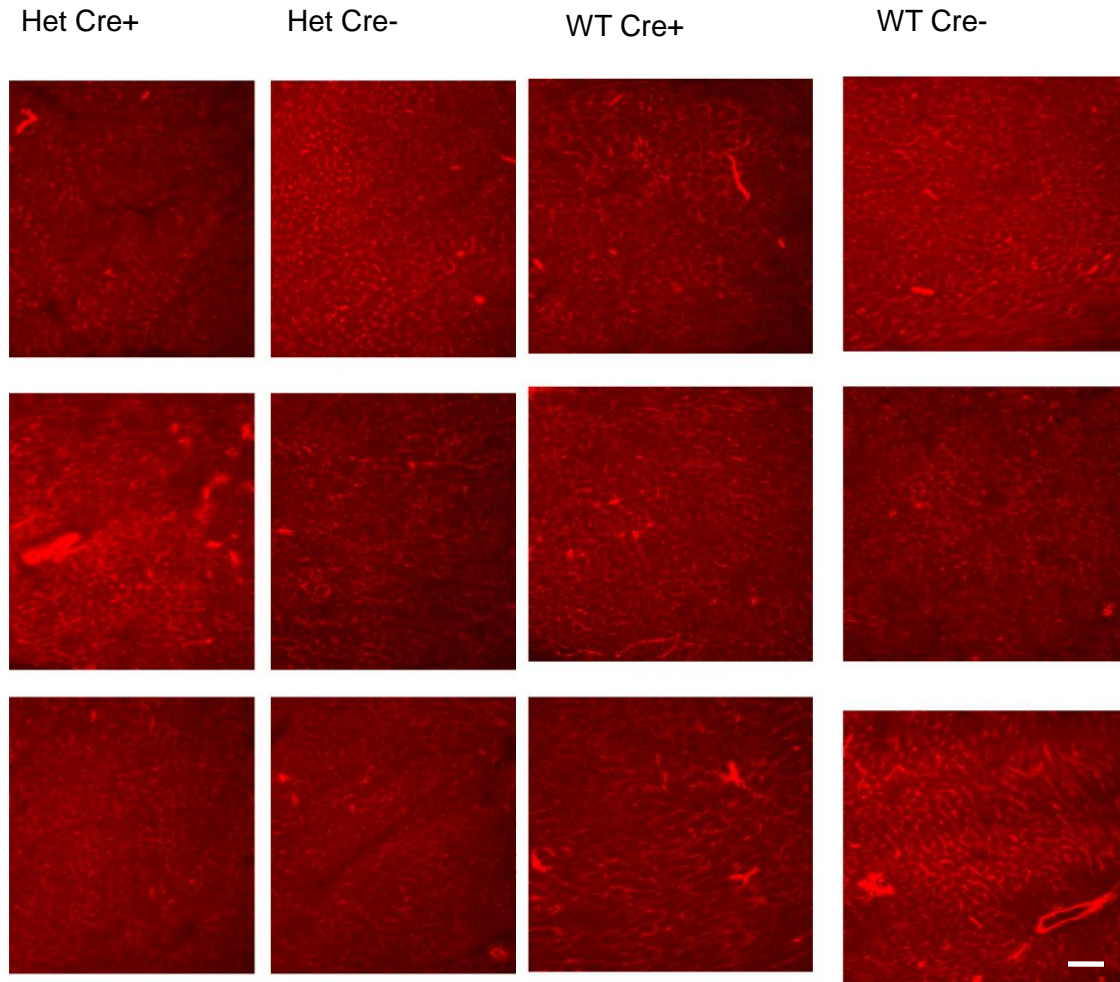


**Figure 7.** Claudin-5 immunofluorescence staining of heart sections of dobutamine-stressed 25 week-old experimental het cre<sup>+</sup> and control mice hearts. Claudin-5 staining was reduced in the myocardium of dobutamine-stressed experimental het cre<sup>+</sup> mice (n=3) in a mosaic pattern, compared to dobutamine-stressed wt cre<sup>-</sup> (n=4), wt cre<sup>+</sup> (n=4), and het cre<sup>-</sup> (n=3). (Bar equals 100μm)

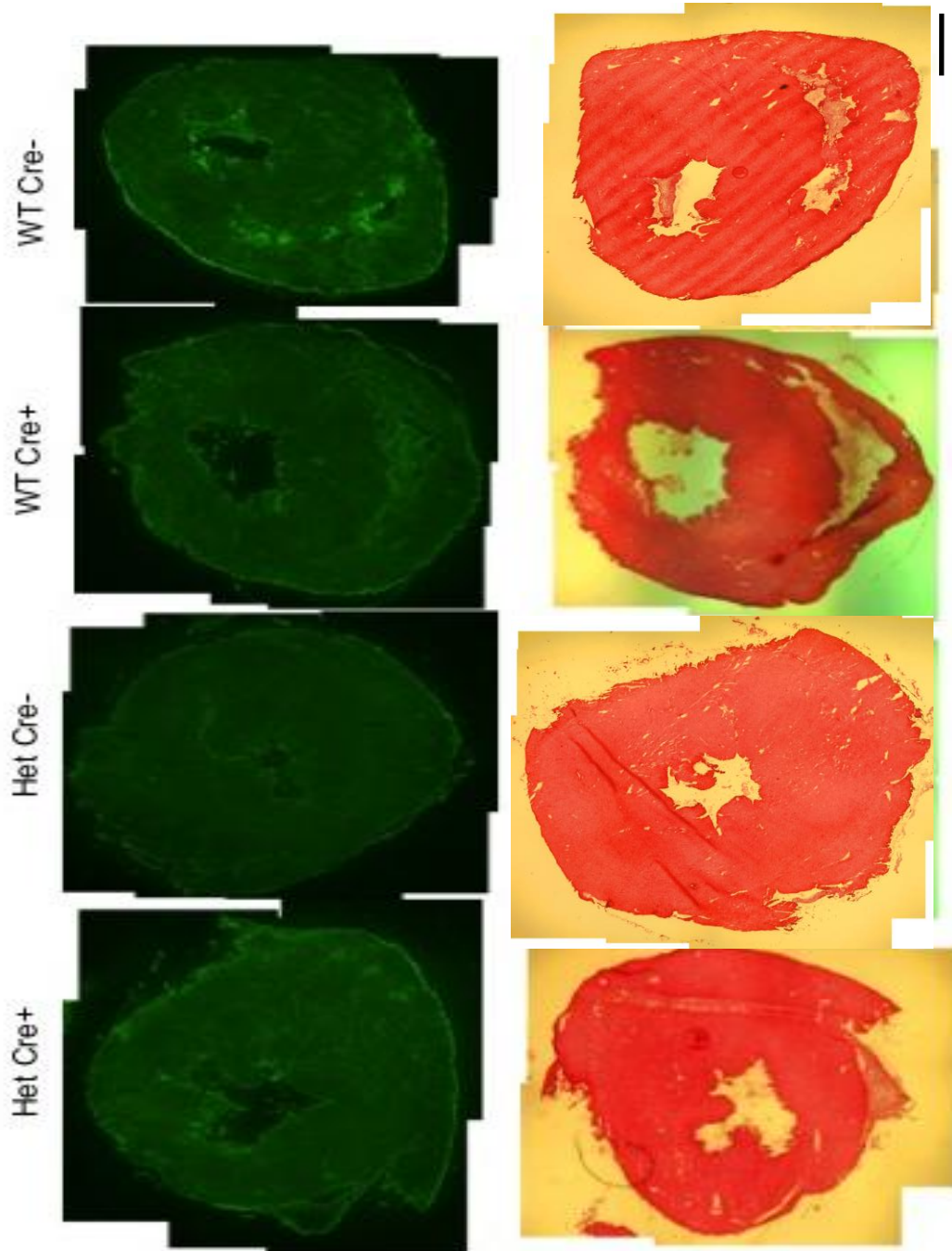


**Figure 8.** Top: IgG staining of composited heart sections of dobutamine-stressed experimental het cre+ mice and controls. IgG immunostaining of transverse sections of whole heart composites shows several regions of damage in experimental het cre+ mice (n=3), compared to wt cre- (n=4), wt cre+ (n=4), and het cre- (n=3), indicating that claudin-5 reductions in dobutamine-stressed het cre+ mice may have resulted in damage to the myocardium. Note that the bright green staining in wt cre- is indicative of vessels. Bottom: Hematoxylin and eosin staining of composited heart sections of dobutamine-stressed experimental het cre+ and control mice. Immunohistochemical staining did not show any signs of dilation or damage to the myocardium consistent with cardiomyopathy. (Bar equals 1mm)

**Results for Aim 2: To determine whether claudin-5 expression helps protect skeletal muscle from the degenerative effects of dystrophin-deficiency.**

**E. Claudin-5 ectopic expression via rAAV6-claudin-5 ( $1 \times 10^{11}$ vg) prevented damage to the muscle membrane in dystrophin-deficient skeletal muscle.**

Four week-old *mdx* mice (Group 1, n=5) were injected with a rAAV6-claudin-5 vector at  $1 \times 10^{11}$  vg in PBS and an equivalent volume of PBS, as the control, via intramuscular injections into the left and right TA muscles, respectively. These mice were dissected at eight weeks of age to ensure that claudin-5 had transduced the maximal amount of skeletal muscle fibers. The injected TA muscles were harvested and studied using immunohistochemical stains to determine if claudin-5 ectopic expression would help prevent damage to the muscle membrane. Claudin-5 (red) immunofluorescence staining of rAAV6-claudin-5-injected TA muscles demonstrated that treatment with this vector is able to transduce skeletal muscle fibers and upregulate claudin-5 expression levels in the *mdx* mouse model (Figure 9A), as compared to the PBS-injected TA muscle (Figure 9D). Merged images of claudin-5 and DAPI (blue) immunofluorescence staining (Figures 9B and 9E) of the injected TA muscles showed that the claudin-5 expressing muscle fibers did not exhibit a large number of fibers with central nuclei, which is a marker of cumulative degeneration and regeneration cycles that indicate damage to the muscle fibers. This data indicates that the upregulation of claudin-5 exhibited protective effects in dystrophin-deficient skeletal muscle because it prevented damage to the muscle membrane. Hematoxylin and eosin staining on these injected TA muscles showed more regions of damage to the skeletal muscle in PBS-injected *mdx* mice (Figure 9F) compared to rAAV6-claudin-5 vector-injected mice (Figure 9C). To serve as an untreated control, the quadriceps muscles on rAAV6-claudin-5- and PBS-injected legs were also harvested and stained with claudin-5 and DAPI to demonstrate the lack of high-expressing claudin-5 fibers in untreated dystrophin-deficient skeletal muscles (data not shown). The lack of high-expressing claudin-5 fibers in the quadriceps muscle of the rAAV6-claudin-5 vector-injected leg also confirms that the



expression of the vector from the intramuscular injection was localized to the site of injection, indicating that this procedure is specialized to primarily target only the injected muscle.

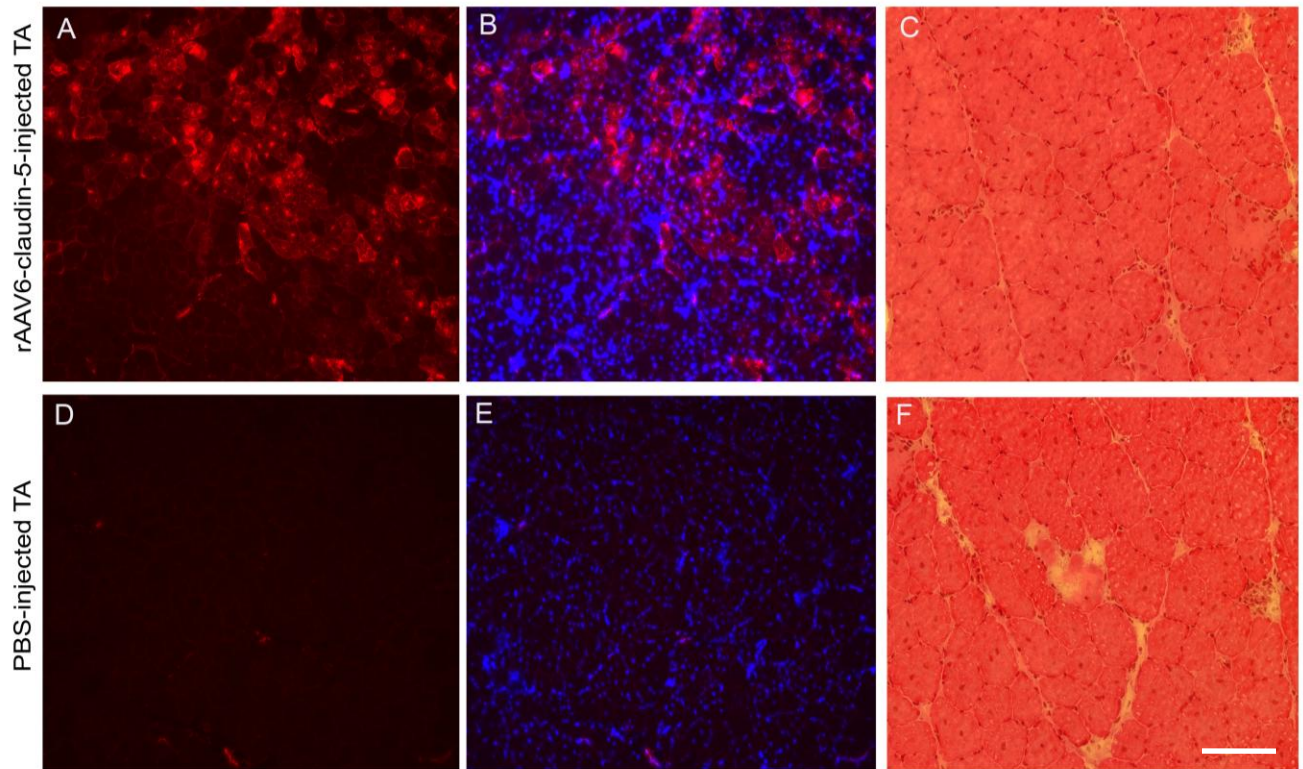


**Figure 9.** Immunohistochemical staining of rAAV5-claudin-5 vector ( $1 \times 10^{11}$  vg) and PBS treated dystrophin-deficient TA muscles at eight weeks of age. A) Claudin-5 immunofluorescence staining showed that rAAV6-claudin-5 vector at  $1 \times 10^{11}$  vg injected into TA muscles of *mdx* mice transduced a majority of muscle fibers. B) Merged claudin-5 (red) and DAPI (blue) immunofluorescence stained-TA muscles of *mdx* mice at eight weeks of age injected with rAAV6-claudin-5 vector at  $1 \times 10^{11}$  vg showed that the claudin-5 expressing fibers in rAAV6-claudin-5-treated skeletal muscle did not exhibit a large number of fibers with central nuclei, a marker of damage to the skeletal muscle. C) Hematoxylin and eosin staining on TA muscles of *mdx* mice injected with rAAV6-claudin-5 vector at  $1 \times 10^{11}$  vg showed few regions of damage to the skeletal muscle. D) Claudin-5 immunofluorescence staining showed a lack of claudin-5 expressing muscle fibers in PBS-injected TA muscles of *mdx* mice, which indicated the proof-of-principle that the rAAV6-claudin-5 vector upregulated claudin-5 expression in dystrophin-deficient skeletal muscle. E) Merged claudin-5 and DAPI immunofluorescence stained-TA muscles of *mdx* mice at eight weeks of age injected with PBS showed a large number of fibers with central nuclei. F) Hematoxylin and eosin staining on TA muscles of *mdx* mice injected with PBS showed more regions of damage, indicated by necrosis of myocytes and increased fibrosis, to the skeletal muscle in PBS-injected *mdx* mice at eight weeks of age compared to rAAV6-claudin-5 vector-injected *mdx* mice (C). These results indicated that the upregulation of claudin-5 prevented damage to the muscle membrane. (Bar equals 100 $\mu$ m)

**F. rAAV6-claudin-5 transduced more dystrophin-deficient skeletal muscle fibers at a dose of  $5 \times 10^{11}$  vg.**

The rAAV6-claudin-5 vector was injected into the left and right TA muscles of each mouse at  $5 \times 10^{11}$  vg and  $1 \times 10^{12}$  vg, respectively, in four week-old *mdx* mice (Group 2, n=2) in order to test which dose achieved the highest or complete transduction of claudin-5 in TA muscle fibers. The mice were dissected at eight weeks of age, and the injected TA muscles were harvested. Whole TA muscle composites of claudin-5 immunofluorescence staining (Figure 10) showed that rAAV6-claudin-5 vector at  $5 \times 10^{11}$  vg exhibited a high number of claudin-5 expressing muscle fibers. Quantitation of central nuclei via claudin-5 and DAPI immunofluorescence staining showed that this dose also maintained the highest number of claudin-5 expressing muscle fibers without central nuclei. These results indicated that administration of rAAV6-claudin-5 vector to dystrophin-deficient skeletal muscle at a dose of  $5 \times 10^{11}$  vg transduced the highest amount of muscle fibers in which claudin-5 expression prevented damage to dystrophin-deficient skeletal muscle.

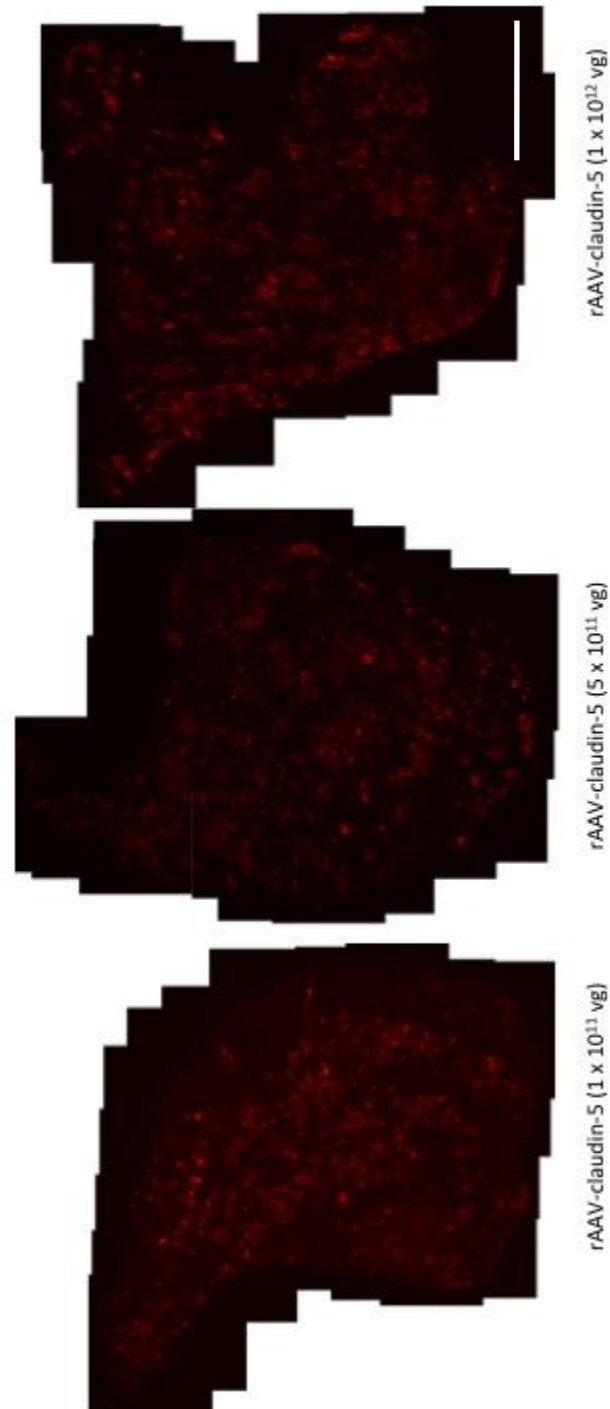


**Figure 10.** Claudin-5 immunofluorescence staining of TA muscles of *mdx* mice at eight weeks of age injected with rAAV6-claudin-5 vector at  $1 \times 10^{11}$  vg,  $5 \times 10^{11}$  vg, and  $1 \times 10^{12}$  vg, respectively. *Mdx* mice injected with rAAV6-claudin-5 vector at  $5 \times 10^{11}$  vg exhibited the highest number of claudin-5 (red) expressing skeletal muscle fibers without central nuclei. (Bar equals 1mm)

**G. Increased claudin-5 expression via rAAV6-claudin-5 ( $5 \times 10^{11}$  vg) prevented cumulative degeneration and regeneration cycles and maintained skeletal muscle integrity in dystrophin-deficient skeletal muscle.**

Upon confirming that the rAAV6-claudin-5 vector at  $5 \times 10^{11}$  vg transduced the highest amount skeletal muscle fibers without central nuclei, the vector was administered at this dose to additional four week-old *mdx* mice (Group 3). These mice were dissected at eight weeks of age, and the injected TA muscles were harvested. Whole composites of claudin-5 (red) and DAPI (blue) immunofluorescence stains (virus-injected: Figure 11A and PBS-injected: Figure 11C) on TA muscles of *mdx* mice injected with rAAV6-claudin-5 vector at  $5 \times 10^{11}$  vg showed that the rAAV6-claudin-5 vector transduced approximately 70% of dystrophin-deficient skeletal muscle fibers, and further that only 22% of claudin-5 expressing skeletal muscle fibers contained cumulative regeneration and degeneration cycles indicative of fiber damage, compared to 48% in PBS-injected *mdx* mice at eight weeks of age. The overall lack of central nuclei in claudin-5 expressing fibers in rAAV6-claudin-5 vector-injected TA dystrophin-deficient muscles compared to PBS-injected TA muscles was shown to be statistically significant ( $p=0.00663$ ) using a one-way ANOVA, supporting the hypothesis that claudin-5 ectopic expression helps compensate for dystrophin-deficiency in skeletal muscle. Whole composites of anti-mouse IgG immunofluorescence stains (virus-injected: Figure 11B and PBS-injected: Figure 11D) on TA muscles of *mdx* mice treated with rAAV6-claudin-5 vector at  $5 \times 10^{11}$  vg and PBS indicated a lack of major muscle membrane damage in skeletal muscle at eight weeks of age. These results indicated that claudin-5 expression maintained skeletal muscle integrity and prevented damage to muscle fibers in dystrophin-deficient skeletal muscle.



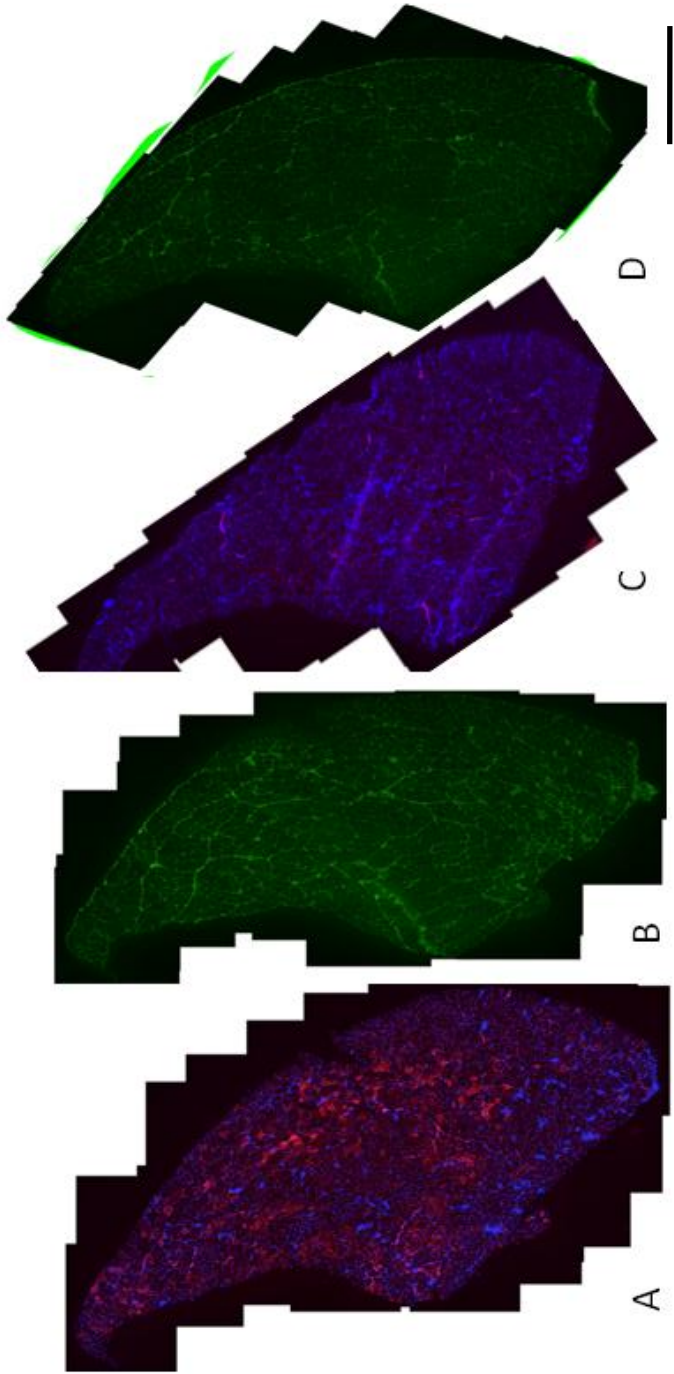


**Figure 11.** Immunofluorescence staining of TA muscles of *mdx* mice of rAAV6-claudin-5 vector at  $5 \times 10^{11}$  vg and PBS injected treatment groups. A) Composite of claudin-5 (red) and DAPI (blue) immunofluorescence staining of TA muscles of *mdx* mice injected with rAAV6-claudin-5 vector at  $5 \times 10^{11}$  vg showed that this dose transduced approximately 70% of muscle fibers and further demonstrated that only 22% of claudin-5 expressing skeletal muscle fibers contained central nuclei. C) Composite of claudin-5 and DAPI immunofluorescence staining of TA muscles of *mdx* mice injected with PBS demonstrated that 48% of muscle fibers contained central nuclei at eight weeks of age. C) Composite of anti-mouse IgG immunofluorescence staining of TA muscles of *mdx* mice injected with rAAV6-claudin-5 vector at  $5 \times 10^{11}$  vg indicated a lack of major muscle membrane damage at eight weeks of age. D) Composite of IgG immunofluorescence staining of TA muscles of *mdx* mice injected with PBS also indicated a lack of major muscle membrane damage at eight weeks of age. One way-ANOVA revealed that TA muscles of *mdx* mice injected with rAAV6-claudin-5 vector at  $5 \times 10^{11}$  vg exhibited significantly less central nuclei than PBS-injected TA muscles of *mdx* mice, which indicated that the virus prevent muscle membrane damage in dystrophin-deficient skeletal muscle at eight weeks of age. (Bar equals 1mm)

## **VIII. Discussion**

### **Discussion for Aim 1: To determine whether claudin-5 reduction in cardiomyocytes is sufficient to cause cardiomyopathy.**

This experiment identifies initial signs of compromised cardiac function indicative of the onset of a cardiomyopathic phenotype and simultaneous reductions in the claudin-5 protein in a claudin-5 knockdown mouse model. While claudin-5 reduction in the myocardium has not yet caused significantly reduced ejection fractions or definitive histological hallmarks of cardiomyopathy in the experimental mice compared to the controls, early indications of a cardiomyopathic phenotype have been identified by reduced ejection fractions of experimental het cre<sup>+</sup> mice at 23 weeks post-tamoxifen treatment. An additional study to gather longitudinal echocardiogram data is currently being conducted in order to determine the timepoint at which het cre<sup>+</sup> mice exhibit a significant reduction in ejection fraction as a result of loss of claudin-5. This data and its future implications support the hypothesis that claudin-5 may be necessary to maintain normal heart function and the integrity of the myocardium.

The slow development of compromised cardiac function in het cre<sup>+</sup> mice treated with tamoxifen chow presented in this study mimics the gradual development of cardiomyopathy in humans, confirming that mice treated with tamoxifen chow to induce claudin-5 reduction is more representative of the proper timepoints observed in the development and progression of DCM. A previous study of tamoxifen-injected mice showed reduced ejection fractions of het cre<sup>+</sup> and wt cre<sup>+</sup> mice. This indicated that tamoxifen injections resulted in a cre-dependent toxicity, which compromised whole heart function as apparent with the reduced ejection fractions of the cre<sup>+</sup> groups. To alleviate the toxicity evident with tamoxifen injections, this study treated mice with

tamoxifen chow, administered at a lower dose per day and over a longer period of time. Echocardiograms of 14 week-old mice treated with tamoxifen chow showed that het cre<sup>+</sup> mice had lower ejection fractions than any other genotype of tamoxifen-chow treated mice, yet it was higher than tamoxifen-injected mice of the same age, indicating the elimination of the cre-dependent toxicity. The observation that tamoxifen chow-treated het cre<sup>+</sup> mice develop a cardiomyopathic phenotype at a slower rate than tamoxifen-injected mice, combined with PCR analysis comparing the two groups, further confirmed that tamoxifen chow administration was a viable treatment because it avoided the toxic effects apparent with tamoxifen injections.

The strengths of this paper lie in its attempt to determine causation between claudin-5 reductions and the development of DCM in a novel mouse model. While many laboratories study heart failure, few are investigating the claudin-5 protein and its role in the progression of DCM and heart failure. This study identified a cre-dependent toxicity issue with tamoxifen injections and concluded that tamoxifen chow administration is a viable and effective alternative to knockdown claudin-5 expression in the myocardium, which is congruent with results from other publications.<sup>1</sup> This finding has further implications in other mouse models that utilize tamoxifen to activate the cre-lox system to prevent protein expression. This paper also provides promise of a cardiomyopathic phenotype through longitudinal echocardiograms of the experimental mice.

Despite the progression of initial signs of cardiomyopathy in tamoxifen chow-treated mice at 20, 25, and 29 weeks of age, the dobutamine stress test did not induce a cardiomyopathic phenotype in 25 week-old het cre<sup>+</sup> mice. This data is limited because the mice underwent short-term trials, so we will continue to perform longitudinal

echocardiograms on the tamoxifen chow-treated mice with and without stress to determine if they develop significantly reduced ejection fractions as a result of claudin-5 reductions. Future experiments consisting of additional stress tests, longitudinal data from aged mice, or a new mouse model will be necessary to identify if loss of claudin-5 is sufficient to cause cardiomyopathy. Another potential limitation is that the echocardiogram machinery may not be sensitive enough to detect differences in cardiac function in CKD mice. If few differences are found in future measurements from echoes between the het cre<sup>+</sup> and wt cre<sup>-</sup> mice, mice will undergo cardiac MRI on a vertical bore 11.7 Telsa, 30-mm bore magnetic resonance imaging system. This test will examine cardiac function in more quantitative detail than echo data alone and may provide more accurate measurements.

**Discussion for Aim 2: To determine whether claudin-5 expression helps protect skeletal muscle from the degenerative effects of dystrophin-deficiency.**

This experiment provides evidence that treatment with rAAV6-claudin-5 vector in the *mdx* model of muscular dystrophy is able to prevent histological indicators of damage to the skeletal muscle. By increasing the original concentration of the vector administered to the skeletal muscle by 5-fold, there was an improvement in the total number of fibers transduced in the TA muscle and an additional statistically significant decrease in the amount of centrally nucleated fibers in the rAAV6-claudin-5 vector-treated skeletal muscles as compared to the controls. These findings support our hypothesis that claudin-5 ectopic expression helps prevent damage to the skeletal muscle membrane. However, further studies that achieve complete transduction of the skeletal muscle are necessary in order to prove the incontrovertible success of this therapy.

Though the histological indicators of muscle membrane damage in skeletal muscle were improved in rAAV6-claudin-5-treated dystrophic skeletal muscles, there was still evidence of centrally nucleated fibers present after upregulated claudin-5 expression in the muscles. However, there is ongoing damage to the skeletal muscle from three weeks of age in *mdx* mice, and consequently the centrally nucleated fibers observed upon dissection at eight weeks of age could have been damaged before claudin-5 was ectopically expressed. Despite this possibility, the experiment in this study was conducted as such because it is most clinically relevant to DMD patients, who have ongoing damage to their skeletal muscles and are often not diagnosed until muscle damage appears. Further experiments that administer rAAV6-claudin-5 vector to *mdx* mice around birth and delineate the timing of administration are necessary in order to determine if claudin-5 ectopic expression prior to the onset of skeletal muscle

membrane damage is able to prevent cumulative cycles of degeneration and regeneration and maximize its transduction in skeletal muscle fibers.

The strengths of this experiment lie in its attempt to establish the potential therapeutic value of claudin-5. By providing evidence that claudin-5 ectopic expression is able to prevent significant damage to the muscle membrane in dystrophin-deficient skeletal muscle, there is support that upregulating claudin-5 levels could be used to prevent damage to the myocardium, another type of striated muscle, and potentially improve the condition of the heart in patients suffering from DCM. Further experiments additionally will need to identify practical and low-cost ways to pharmacologically administer therapeutic levels of claudin-5 to DMD patients.

This data is limited because the mice were analyzed only via histological indicators of damage. Additional histological and physiological experiments should be conducted to determine if claudin-5 is able to prevent additional indicators of skeletal muscle pathology and assess other effects of claudin-5 ectopic expression. These future experiments will also help identify the mechanism of action of claudin-5 in preventing damage to dystrophic skeletal muscles.

## **IX. Conclusion**

This paper investigated whether reductions in the claudin-5 protein were sufficient to cause cardiomyopathy by first knocking-down cardiac claudin-5 levels in a mouse model and then characterizing the phenotype of this mouse model. After identifying a cre-dependent toxicity in tamoxifen-injected mice, tamoxifen chow was administered to CKD mice and proved to be an effective treatment to knockdown cardiac claudin-5 levels and cause initial signs of a cardiomyopathic phenotype in the CKD mouse model. This supports the hypothesis that cardiac claudin-5 reduction may cause cardiac dysfunction characteristic of the development of DCM, and further characterization of the phenotype of this mouse model at later timepoints may exhibit a clear causative relationship between loss of claudin-5 and the development of DCM.

This paper also studied whether upregulating claudin-5 expression was able to maintain the structural integrity of skeletal muscle in a dystrophin-deficient mouse model. The administration of rAAV6-claudin-5 vector by 5-fold, at  $5 \times 10^{11}$  vg, showed that increased claudin-5 expression significantly prevented cumulative degeneration and regeneration cycles and maintained skeletal muscle integrity in dystrophin-deficient skeletal muscle. This study helps identify claudin-5 as a potential therapeutic target for treating skeletal muscle fibrosis characteristic of DMD.



## **X. References**

1. Anderson, KB, Winer, LH, Mork, HK, Molkentin, JD, Jaisser, F. Tamoxifen administration routes and dosage for inducible cre-mediated gene disruption in mouse hearts. *Transgenic Res*, 2009.
2. Crisp, A. *et al.* Diaphragm Rescue Alone Prevents Heart Dysfunction. *Hum Mol Genet*, 2010.
3. Delfín, DA, Xu, Y, Schill, KE, Mays, TA, Canan, BD, Zang, KE, Barnum, JA, Janssen, PM, and Rafael-Fortney, JA. Sustaining cardiac claudin-5 levels prevents functional hallmarks of cardiomyopathy in a muscular dystrophy mouse model. *Mol Ther*, May 1. doi: 10.1038/mt.2012.81, 2012.
4. Duan, D. *et al.* Challenges and opportunities in dystrophin-deficient cardiomyopathy gene therapy. *Hum Mol Genet* 15 Spec No 2: R253–R261, 2006.
5. Gregorevic P, Blankinship MJ, Allen JM, Crawford RW, Meuse L, Miller DG, Russell DW, and Chamberlain JS. Systemic delivery of genes to striated muscles using adeno-associated viral vectors. *Nat Med* 10: 828-834. Epub 2004 Jul 2025., 2004.
6. Kaspar, RW, Allen, HD and Montanaro, F. Current understanding and management of dilated cardiomyopathy in Duchenne and Becker muscular dystrophy. *J Am Acad Nurse Pract* 21: 241–249, 2009.
7. Mays, T. A. *et al.* Claudin-5 levels are reduced in human end-stage cardiomyopathy. *J Mol Cell Cardiol* 33, 359-371, 2001.
8. Mendell, JR, Schilling, C, Leslie, ND, Flanigan, KM, al-Dahhak, R, Gastier-Foster, J, Kneile, K, Dunn, DM, Duval, B, Aoyagi, A. *et al.* Evidence-based path to newborn screening for Duchenne muscular dystrophy. *Ann Neurol*. 71, 304-313, 2012.

9. Mutoni, F., Torelli, S., and Ferlini, A. Dystrophin and Mutations: One Gene, Several Proteins, Multiple Phenotypes. *Lancet Neurol* 2, 731-40, 2003.
10. Paul S. Ventricular remodeling. *Crit Care Nurs Clin North Am* 15: 407-411, 2003.
11. Sanford JL, Edwards JD, Mays TA, Gong B, Merriam AP, and Rafael-Fortney JA. Claudin-5 localizes to the lateral membranes of cardiomyocytes and is altered in utrophin/dystrophin-deficient cardiomyopathic mice. *J Mol Cell Cardiol* 38: 323-332, 2005.
12. Sohal, DS, Nghiem, M, Crackower, MA, Witt, SA, Kimball, TR, Tymitz, KM, Pennigerm, JM, Molkentin, JD. Temporally regulated and tissue-specific gene manipulations in the adult and embryonic heart using a tamoxifen-inducible cre protein. *Circ Res* June 21. doi: 10.1161/hh1301.092687, 2001.
13. Tinsley, J. M. *et al.* Expression of full-length utrophin prevents muscular dystrophy in *mdx* mice. *Nat Med* 4, 1441-444, 1998.
14. Townsend, D, Yasuda, S, Li, S, Chamberlain, JS and Metzger, JM. Emergent dilated cardiomyopathy caused by targeted repair of dystrophic skeletal muscle. *Mol Ther* 16: 832–835, 2008.